Binary Diol−Water Systems Studied by ^{17}O Nuclear Magnetic Resonance Spectroscopy. Interpretation of the Effect of Diol Structure on ^{17}O-Water Chemical Shift. Formation of Networks of Water Molecules Stabilized by Weak C−H···O Interactions

Roger A. Klein* and Victor Pacheco

Institute for Physiological Chemistry, University of Bonn, Nussallee 11, D-53115 Bonn, Federal Republic of Germany

Received: February 7, 2001; In Final Form: April 27, 2001

The chemical shift for ^{17}O-labeled water in binary diol−water systems shows two types of dependency on mole fraction, determined by the structure of the diol. Type I behavior consists of a single component which is substantially linear and monotonic in the upfield direction with increasing diol concentration and independent of temperature. Type II behavior is biphasic with an initial downfield component which is strongly temperature dependent occurring for glycol mole fractions <0.20, followed at mole fractions ≥ 0.20 by a linear component which may be in either the upfield or downfield direction, analogous to type I behavior. Type II behavior seems to be associated exclusively with diols containing a terminal methylcarbinol group, $CH_3CH(OH)-$, at least for the series of diols studied in this paper. The initial downfield component caused by this group is interpreted in terms of water structuring and the formation of a clathrate-like cage involving 10−15 water monomers stabilized by weak hydrogen bonds around the methylcarbinol group.

Introduction

As part of a wider study into the solution structure of binary diol−water systems as models for carbohydrate−water interactions,[1−4] in this paper we have investigated the effect of an extensive series of homologous diols, at mole fractions between 0.0 and 0.9, on the NMR chemical shift of ^{17}O-labeled water. Changes in the nuclear shielding tensor or in chemical shift reflect the electronic environment or "shielding" experienced by the nucleus. Upfield shifts, in a negative direction as far as chemical shift is concerned, are associated with an increase in the shielding tensor. Conversely, downfield shifts, positive in the sense of chemical shift, result from "deshielding", normally seen for compounds with electron-withdrawing substituents in the vicinity of the resonating nucleus. For light nuclei such as ^1H, deshielding is associated with a decrease in nuclear electron density. This approximation is not generally true for heavier nuclei such as ^{13}C or ^{17}O, and although an alcohol oxygen is deshielded by protonation, the reverse is true for a carbonyl oxygen.

Hydrogen bonding in solution results in downfield NMR chemical shifts (a +ppm effect). Indeed, downfield shifts are often used as evidence of hydrogen-bond formation and thus "structuring", whereas an upfield shift (increased nuclear shielding) is taken as indicating the breaking or weakening of hydrogen bonds, known as "destructuring". $H_2{}^{17}O$ shows a marked downfield shift, both experimentally and in ab initio calculations, on formation of $(H_2O)_n$ complexes. The ^{17}O chemical shift for liquid water at 373 K is some 36−38 ppm downfield from the vapor phase value at the same temperature, with the protons resonating ≈5 ppm downfield.[5,6] Associated with this downfield shift is a marked increase in the electric field gradient (EFG) asymmetry parameter, η, on passing from the vapor phase through the liquid phase to ice.[7] The changes in chemical shift support the concept of an increasingly important paramagnetic contribution, σ^p, as the oxygen atom becomes distorted from spherical symmetry with decreasing temperature. Wu et al.[6] have shown recently, in solid-state ^{17}O NMR studies of the H_3O^+ ion in toluenesulfonate monohydrate (TAM), that the oxygen nucleus is particularly sensitive to hydrogen bonding. In the bound state the H_3O^+ oxygen is ∼40 ppm less shielded than in the free state, a trend observed for other singly bound oxygen atoms. Moreover, Moriarty and Karlström[7] have demonstrated using Monte Carlo simulation that there is a progressive decrease in the magnitude of V_{ZZ}, and hence Q_{CC}, as well as an increase in η from 0.75 to 0.93, as water passes from the unbound state in the gas phase to the strongly bound state in ice.

^{17}O-Labeled water has advantages compared to ^1H_2O for studying solution structure by NMR methods. These include a greatly reduced rate of chemical exchange between water and organic solutes for the ^{17}O nucleus and much larger chemical shifts. Disadvantages include the low natural abundance of this isotope of oxygen, its expense, and quadrupolar broadening of resonances.

We have measured ^{17}O chemical shifts for labeled water in the presence of all the (1,2)-, (α,ω)-, and (α-1),(ω-1)-diols with chain lengths from ethane ($n = 2$) to hexane ($n = 6$), including 2-methyl-1,3-propanediol, as binary diol−water mixtures at temperatures of 313, 328, and 343 K in the range $X_{diol} = 0.0-0.9$.

Two distinct types of behavior are seen. All straight-chain diols, whether (1,2) or (α,ω), give a relationship between the diol mole fraction and chemical shift for the water oxygen atom which consists of a single monotonic component. This single component, which is basically linear, exhibits upfield chemical shifts with increasing diol concentration, often with a small degree of negative curvature (concave toward the *x*-axis), and close to zero temperature dependence. We refer to this type of

* Corresponding author. Telephone: 49 228 73 2422. FAX: 49 228 73 2416.

10.1021/jp010470v CCC: $20.00
Published on Web 09/19/2001

behavior as type I behavior. On the other hand, diols containing (α-1) and/or (ω-1) methyl groups but not longer alkyl groups, show a two-component response, starting with 1,2-propanediol. The initial component is approximately exponential and in the downfield direction followed by a subsequent upfield linear component, corresponding to type I behavior. The downfield component, which results in a minimum appearing at an X_{diol} value between 0.0 and 0.2, is strongly temperature dependent, in contrast to the linear component; the downfield component has an amplitude approximately proportional to the number of methyl groups present. We refer to this two-component behavior as type II behavior. Type II behavior is associated with the presence of a $CH_3CH(OH)-$ group in the series of diols studied here. The different temperature sensitivities for the exponential and linear components suggest that different physical mechanisms are operative.

We interpret type I and type II behavior in this paper in terms of possible molecular interactions for the various binary diol−water mixtures, especially in the dilute region where $X_{diol} \leq 0.1$, and the way that these may affect aqueous solution structure, as a system average as well as close to the diol itself. We postulate a clathrate-like cage involving 10−15 water molecules around the $CH_3CH(OH)-$ group stabilized by weak hydrogen bonds as an explanation for the initial downfield component seen in type II behavior.

Materials and Methods

All the diols used were obtained as anhydrous substances of the highest purity available commercially from either Sigma-Aldrich or Fluka. Purity was usually ≥98%. Where purity was less than this or the diol was known not to be completely dry, fractional distillation in vacuo was employed to remove water or impurities, mainly structural homologues.

^{17}O NMR spectroscopy was carried out in high-precision 5 mm glass tubes, with an external $H_2{}^{17}O/D_2O$ reference and lock standard in the form of a coaxially mounted capillary inside the NMR tube, using a Bruker AMX-500 spectrometer at 67.784 MHz with a Spectrospin VSP-500 variable-frequency mulit-nuclear inverse receiver head. A small amount of ^{17}O-enriched water (∼25 μL at 25% isotopic enrichment) was added to each sample to improve the signal-to-noise ratio and to reduce acquisition times; allowance was made for this additional water in calculating the mole fraction. Measurements were made at temperatures of 313, 328, and 343 ± 0.5 K to avoid problems associated with high sample viscosity. Chemical shifts were determined using the internal capillary as reference by interpolating the peak position on screen using the cursor; ^{17}O shifts were reproducible ±0.05 ppm in the long term for measurements carried out on individual samples. Samples of known mole fraction were prepared by weight not volume, resulting in reproducibility for chemical shifts for a particular mole fraction of better than ±1% or ±0.05 ppm over many months.

Nonlinear curve fitting was carried out using the Levenberg−Marquardt method, switching between an initial steepest linear descent followed by the Gauss−Newton or inverse-Hessian method as the minimum is approached, as implemented in the GraphPad Prism software package.[8−10]

Results

The following diols all show single-component linear, or nearly linear type I behavior: ethane-1,2-diol (12EG), butane-1,2-diol (12BD), pentane-1,2-diol (12PD), hexane-1,2-diol (12HD), propane-1,3-diol (13PG), butane-1,4-diol (14BD), pentane-1,5-diol (15PD), hexane-1,6-diol (16HD), and 2-methyl-propane-1,3-diol (2M13PG). Examples of type I behavior are shown for ethane-1,2-diol and butane-1,4-diol in Figure 1. All the other diols studied showed two-component type II behavior, namely, propane-1,2-diol (12PG), butane-1,2-diol (12BD) (only at lower temperatures, see below), butane-1,3-diol (13BD), D-(−)-butane-2,3-diol (d23BD), *meso*-butane-2,3-diol (m23BD), pentane-2,4-diol (24PD), and hexane-2,5-diol (25HD). Figure 2 shows data for butane-1,3-diol (one terminal methyl group) and *meso*-butane-2,3-diol (two terminal methyl groups). Figure 3 shows similar data for pentane-2,4-diol and hexane-2,5-diol.

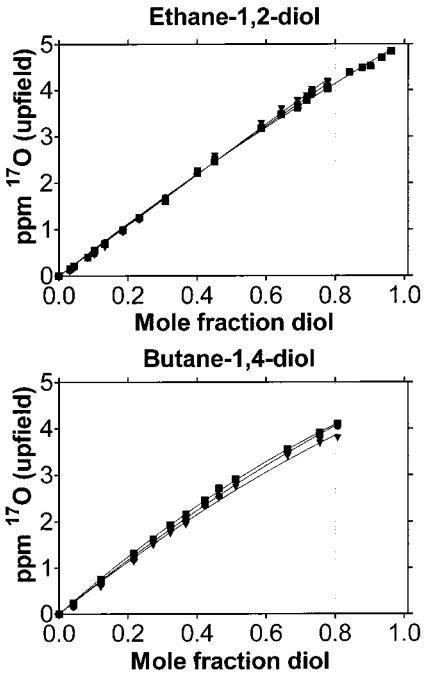

Figure 1. Type I diols. Plots of mole fraction diol against the chemical shift of ^{17}O-water at three temperatures, 313 (▼), 328 (●), and 343 K (■), for ethane-1,2-diol and butane-1,4-diol, both of which are type I diols. Experimental data were fitted with a quadratic function (eq 1) as described in the text.

Experimental data for diols exhibiting type I dependence between mole fraction and chemical shift were fitted with a quadratic expression, in which the *B* coefficient represents the deviation from linearity.

$$y = Ax + Bx^2 \tag{1}$$

Data for type II diols were fitted with a two-component function consisting of an exponential part and a linear part. The initial downfield part of the curve was fitted using an exponential as a mathematical construct solely in order to determine an amplitude for the effect and a normalized gradient at infinite dilution for the glycol; i.e., the limit of the gradient as X_{diol} tends to zero.

$$y = Ee^{-x/K} + Fx \tag{2}$$

The exponential coefficient *K* in eq 2 represents the diol mole fraction at which the initial downfield shift has reached [1 − (1/e)], i.e., 63.2% of its maximum amplitude. The limiting normalized gradient as $X_{diol} \rightarrow 0$ is given by $-1/K$, the reciprocal of the apparent mole fraction at which water and glycol are in the stoichiometric ratio. The stoichiometric ratio for water to glycol N^{GW} at infinite dilution is, therefore, given by

$$N^{GW} = \frac{1 - K}{K} \tag{3}$$

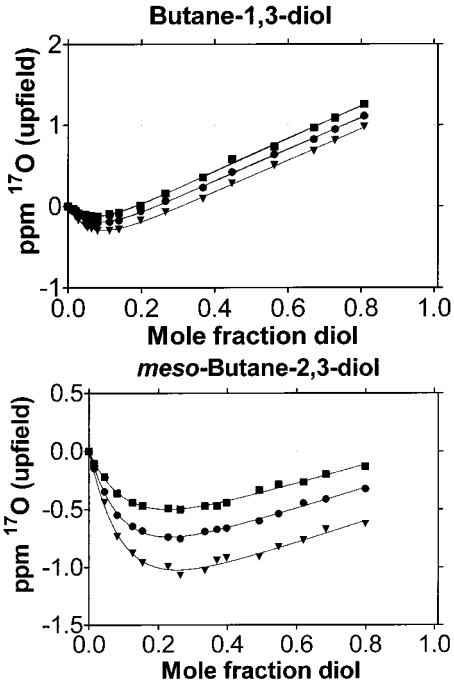

Figure 2. Type II diols (a). Plots of mole fraction diol against the chemical shift of ^{17}O-water at three temperatures, 313 (▼), 328 (●), and 343 K (■), for butane-1,3-diol and *meso*-butane-2,3-diol, both of which are type II diols. Experimental data were fitted with a two-component function consisting of an exponential and a linear part (eq 2) as described in the text.

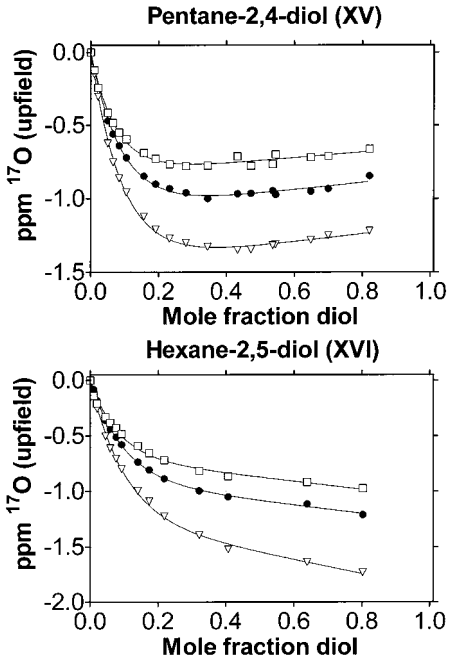

Figure 3. Type II diols (b). Plots of mole fraction diol against the chemical shift of ^{17}O-water at three temperatures, 313 (▽), 328 (●), and 343 K (□), for pentane-2,4-diol and hexane-2,5-diol, both of which are type II diols. Experimental data were fitted with a two-component function consisting of an exponential and a linear part (eq 2) as described in the text.

The reaction would be expected to be first order with respect to diol concentration in this region since water is in excess; i.e., the diol solution is effectively dilute. Moreover, in dilute solution the mole fraction, or molality, and concentration are directly proportional to one another. The initial slope, i.e., at infinite dilution for the diol, gives the limiting number of water molecules associating with the diol in this region. The second part of the curve is fitted as a straight line, based on the experimental data. The use of an exponential is a mathematical convenience. It should not be taken to imply anything about the mechanism of interaction between water and glycol. Irrespective of the appropriate model for this interaction, this procedure provides a measure of the amplitude of the downfield shift and stoichiometric ratio of water to glycol at infinite dilution. Nor should the use of a straight line for the second part of type II behavior be taken to imply ideal two-state behavior, rather that only the experimental data approximate a straight line.

The mole fraction range can be divided into three broad regions: regions I and III correspond to X_{diol} of less than 0.1 and more than 0.9, respectively, i.e., where the solution is dilute with respect to either diol or water; region II is in the middle of the range, with X_{diol} values between 0.1 and 0.9, in which interactions are generally too complex to be analyzed.

The curvature shown by some type I diols results in an intercept on the *y*-axis at $X_{diol} = 1.0$ representing a fractional deviation from linearity of *B*/*A*. The simplest and most trivial explanation for a small negative *B* coefficient would be that the diol used was contaminated with water. If this were the case, the quotient *B*/*A* would be determined by the weight fraction of water, α, in the apparently anhydrous diol, by the following expression:

$$B/A = 1 - \frac{1}{1 - R^{DW}\left(\frac{\alpha}{1-\alpha}\right)} \qquad (4)$$

where R^{DW} is the ratio of the molecular weight of the diol to that of water. The negative *B* coefficients observed could be explained by contamination with 5−7% w/w water. This explanation is, however, unlikely since all the diols used were either anhydrous from freshly opened bottles or freshly distilled. Direct measurement of the water uptake by an unstirred, open sample of ethane-1,2-diol standing at room temperature, with an area/volume ratio comparable to that of an NMR tube, showed that 1.0−1.5 mg cm^{-2} h^{-1} water was taken up. Thus it would have taken approximately 24 h to increase the water content of the diol by 1% w/w. Moreover, the NMR results were reproducible with ±1% from one experiment to the next, even when the samples had been kept for weeks, suggesting that the deviation from linearity was real and not an artifact caused by the diol being wet but resulting from second-order solute−solvent effects. Some of the more hydrophobic diols showed positive *B* coefficients, i.e., curvature convex to the *x*-axis. Also, all *B* coefficients had a strong dependence on temperature, suggesting their origin as an interaction between diol and water, probably involving hydrogen bonding. Further interpretation of the *B* coefficients in terms of solute−solvent interactions is, however, not justified in the midrange of diol mole fractions (region II).

Type I and Type II Behavior. The coefficients and their standard errors obtained by fitting the experimental data for either type I or type II behavior using eq 1 or 2, are shown for all the diols studied in Table 1 at 343 K. All of these compounds were also measured over the full mole fraction range at 313 and 328 K (full data not shown). Type I diols have been listed in order of decreasing magnitude for the limiting slope at infinite dilution of glycol in water, corresponding to coefficient *A* in eq 1. Table 2 lists the estimated mole ratio of water to diol estimated from the initial slope of the downfield component for type II diols, derived as explained above using eq 2. The

TABLE 1: Coefficients Obtained by Fitting Experimental Data of Diol Mole Fraction against Chemical Shift at 343 K Using Either Eq 1 (Type I) or Eq 2 (Type II)

Coefficients for eq 1		
type I diol	A	B
16HD	8.84 ± 0.21	−0.077 ± 0.073
2M13PG	7.39 ± 0.06	−0.214 ± 0.010
15PD	7.02 ± 0.10	−0.290 ± 0.017
14BD	6.57 ± 0.06	−0.278 ± 0.012
13PG	6.08 ± 0.06	−0.211 ± 0.011
12EG	5.75 ± 0.10	−0.125 ± 0.019
12BD	3.29 ± 0.05	−0.090 ± 0.018
12PD	3.54 ± 0.06	−0.242 ± 0.019
12HD	1.68 ± 0.04	0.447 ± 0.039

Coefficients for eq 2			
type II diol	F	E	K
12PG	2.70 ± 0.02	0.487 ± 0.011	0.078 ± 0.003
13BD	2.03 ± 0.03	0.388 ± 0.019	0.062 ± 0.006
r23BD	0.90 ± 0.03	0.780 ± 0.020	0.090 ± 0.004
m23BD	0.83 ± 0.04	0.773 ± 0.026	0.103 ± 0.006
d23BD	0.86 ± 0.03	0.666 ± 0.019	0.087 ± 0.005
24PD	0.19 ± 0.04	0.837 ± 0.024	0.074 ± 0.004
25HD	0.37 ± 0.07	0.691 ± 0.042	0.082 ± 0.009

[a] Abbreviations for diols are found under Results. R23BD, M23BD, and D23BD refer to, respectively, the racemate, the meso form, and the D-(−)-form of 2,3-butanediol.

TABLE 2: Number of Water Molecules, $N(H_2O)$, Interacting with Each Diol Molecule at Infinite Dilution of Diol ($X_{diol} = 0.0$) and 343 K Determined from the Initial Slope, $-1/K$, of the Downfield Component in Type II Behavior

diol	$N(H_2O)$
12PD	11.82 ± 0.45
13BD	15.13 ± 1.46
r23BD	10.11 ± 0.45
m23BD	8.71 ± 0.51
d23BD	10.49 ± 0.60
24PD	12.51 ± 0.68
25HD	11.20 ± 1.23
average	11.42 ± 2.04

stoichiometric ratio for this water/diol interaction was found to be 11.42 ± 2.04 at 343 K; at 313 and 328 K corresponding values were 11.02 ± 2.37 and 11.01 ± 2.57, respectively, demonstrating complete lack of temperature sensitivity. The amplitude of the exponential component in type II behavior was quite strongly temperature dependent, increasing as the temperature was reduced and proportional within experimental error to the number of $CH_3CH(OH)-$ groups present. The linear component for both type I and type II behaviors was essentially independent of temperature as shown using Arrhenius plots, as discussed below. 1,2-Butanediol shows behavior intermediate between type I and type II, with a downfield component only becoming visible at low temperature; it was difficult to fit this portion accurately. Contamination of the butane-1,2-diol with 1−2% of the 1,3-isomer would be sufficient to explain this behavior.

Temperature Sensitivity. Arrhenius plots ($1/T$ versus ln(slope)) for the shorter chain type I and type II diols showed that the linear component characteristic of type I behavior had a very low temperature coefficient not generally statistically different from zero. With the exception of some diols containing five or six carbons atoms, i.e., the pentane and hexane derivatives 12PD, 12HD, 24PD, and 25HD but not 15PD or 16HD, all the other type I and type II diols exhibited A or F coefficients that were effectively independent of temperature with $\Delta H \approx \pm 1$ kcal/mol, i.e., not significantly different from zero. Pentane-1,2-diol and hexane-1,2-diol, however, showed increasing endothermic temperature dependence for the limiting slope, with ΔH equal to 5.2 ± 0.4 and 13.5 ± 2.8 kcal/mol, respectively, probably associated with the increasingly apolar nature of the side chain. The limiting slope for both pentane-2,4-diol and hexane-2,5-diol was slightly exothermic with $\Delta H = -3.3 \pm 0.6$ kcal/mol. There was also a general reduction in limiting slope with increasing chain length, especially for 12HD as well as 25HD, for which it is actually slightly negative (Table 1).

The exponential coefficient, K, for the initial downfield component of type II behavior also showed very low temperature sensitivity ($\Delta H < \pm 0.7$ kcal/mol) not significantly different from zero within experimental error. Again pentane-2,4-diol and hexane-2,5-diol were the exceptions, being slightly exothermic with $\Delta H \approx -1.5 \pm 0.7$ kcal/mol, although given the caveat that measurements were made at only three temperatures even these slopes cannot be considered to be significantly different from zero. On the other hand, however, the amplitude of the exponent and hence the depth of the downfield minimum observed for type II diols was quite strongly temperature dependent and exothermic with ΔH in the range −3 to −4 kcal/mol (−13 to −17 kJ/mol). All of the type II diols gave extremely good linear relationships between $1/T$ and ln(amplitude) with slopes that were statistically significant and very similar to one another. The temperature dependence of the amplitude did not appear to be notably structure dependent: 12PG = −3.3 ± 0.1 kcal/mol, 13BD = −3.1 ± 0.1 kcal/mol, m23BD = −4.0 ± 0.1 kcal/mol,and rac23BD = −4.1 ± 0.9 kcal/mol.

The Arrhenius analysis quite clearly identifies two separate interaction processes between water and diol, within the limitations on interpretation imposed by measurements at only three temperatures. One, the linear type I component, is substantially independent of temperature, at least for the shorter chain diols and all the (α,ω)-diols. The other, the initial downfield exponential characteristic of type II behavior, is markedly exothermic as far as the amplitude but not the stoichiometry is concerned, suggesting that hydrogen bonding which becomes stabilized at lower temperatures may be involved.

Discussion

It has long been known that certain low molecular weight solutes, especially nonelectrolytes containing oxygen, when added to water at low concentrations appear to be able to cause enhancement of water−water hydrogen bonding as judged from the downfield shifts seen for proton NMR data.[11] *tert*-Butyl alcohol (TBA) is particularly effective in this respect and has been extensively studied. Anderson and Symons[12] reported that TBA−water mixtures show a minimum for the water ^{1}H NMR downfield shift with $X_{diol} = 0.04-0.05$, deepening with reduction in temperature, and followed by an upfield shift at higher mole fractions, similar to our results for type II diols. The region where $X_{diol} = 0.04-0.05$ is also associated with discontinuities in ultrasound absorption, IR, UV, and ESR measurements, as well as with hydration kinetics for Co and Fe complexes.[13,14] The NMR downfield shift effect, typified by TBA−water binary mixtures, was interpreted by these authors as showing structuring of solvent water with enhancement of hydrogen bonding between water molecules and the formation of a clathrate-like cage. Visser et al.[15] have noted anomalous behavior for both the apparent molal heat capacity, which is especially sensitive to structural changes in solution, and the molal volume in the

dilute region for TBA−water mixtures, ascribing this behavior not to the OH group but to hydrophobic effects. On structural grounds we would expect TBA to behave in a type II fashion, because of its similarity to the methylcarbinols studied here.

What previous work has not done is to examine systematically the mechanism by which this stabilization of water structure and hydrogen bonding by these small nonelectrolytes could occur, by determining quantitative structure−activity relationships (QSAR) for a series of structurally closely related solutes. Thermodynamic arguments invoking the "hydrophobic effect" and entropy merely serve to confirm that this loose, clathrate-like structure consisting of hydrogen-bonded water molecules is stabilized thermodynamically.[16] In this paper we attempt to provide a plausible *mechanistic* explanation for the enhancement of water−water and water−solute interactions based on what is now known about so-called "weak" hydrogen bonds and on H-bond acceptor or donor activity, derived from experimental data and theoretical ab initio calculations on NMR shielding for a complete series of structurally related diols in binary diol−water systems. We have, for the first time, identified a specific structural entity, the $CH_3CH(OH)-$ group, which is associated with this enhancement of the water−water interaction, finding that diols fall into two functional and structural groups, those that are incapable of causing the downfield shift and which do not contain the methylcarbinol group (type I), and those that can, all of which contain the group (type II).

Two aspects of the data described above need to be discussed. First is the dependence on diol structure of the slope of the mainly linear upfield component and the value of this slope extrapolated to infinite diol dilution; second is the interpretation of the initial downfield exponential component seen for type II diols.

As can be seen from Table 1, coefficient *A*, the limiting slope at zero diol concentration for type I behavior, is strongly dependent on diol structure. A shift upfield suggests breaking of water structure by either weakening the hydrogen bonds between water molecules on average, or by reducing water cluster size. The most simplistic explanation of the linear component characteristic of type I behavior is that water molecules exist in two states or environments, with the proportion of each directly proportional to mole fraction; the first is complexed as "normal" liquid water and the second as isolated molecules interacting with excess diol. From within the data for homologous diols, certain generalizations can be drawn: (i) For the (α,ω)-diols, with $n = 2-5$, there is a general proportionality between the reduction in static dielectric constant from 41.4 for ethane-1,2-diol to 26.2 for pentane-1,5-diol,[17] associated with increased chain length, and an increase in the limiting slope, *A*, with a marked positive discontinuity for $n = 6$, possibly due to the phase behavior of hexane-1,6-diol in water (data not shown). (ii) For the 1,2-diols, however, both the limiting slope, *A*, and dielectric constant decrease with increasing chain length. (iii) All of the (α-1)/(ω-1)-diols, which show type II behavior, give low or even negative limiting slopes, *F*, despite dielectric constants in the range 25−30. Great caution must be exercised, however, in attempting any interpretation of the slope of the linear component for the (α-1)/(ω-1)-diols, all of which show type II behavior, since the solutions are no longer dilute with respect to either diol or water. The situation is bound, however, to be considerably more complex since it is known that glycols can form hydrogen-bonded complexes with water; ethane-1,2-diol gives rise to a eutectic mixture with water at a mole fraction of 0.5 (1:1).[18]

Thus it seems unlikely that the environment of water molecules in the presence of excess diol, and hence the limiting slope, is primarily affected by the dielectric constant. The (α,ω)-diols become more effective at breaking water structure, as evidenced by the upfield shift, as the separation of the terminal hydroxyl groups increases. On the other hand, in the 1,2-diols, where the hydroxyl spacing remains constant, increasing alkyl chain length (or bulk) appears to reduce the structure-breaking activity. The overall effect of the (α-1)/(ω-1)-diols, especially for those containing two methyl groups, i.e., 23BD, 24PD, and 25HD, is to cause structuring as indicated by the net downfield shift at all the mole fractions examined.

Previous studies have used both changes in chemical shift and in relaxation rate to investigate hydration phenomena for ionic and nonionic electrolytes.[5,19] As reported by Bagno et al.,[19] nonelectrolytes show positive *B* coefficients for ^{17}O T_1 relaxation measurements with the exception of urea, formamide, and acetamide. Fister and Hertz[5] have compared the effects of trimethyl- and tributylammonium bromides on both chemical shift and relaxation time in terms of structuring and destructuring effects. Traditionally, ^1H and ^{17}O relaxation rate studies have been used because these are seen to yield a parameter connected more directly with solvent motion. Fewer studies have concentrated on ^{17}O shielding tensors and chemical shifts. More interest, however, is now being shown in the shielding tensors for ^{17}O acting as either a proton acceptor or donor in hydrogen bonds, paralleling increased interest in ab initio quantum mechanical calculations for the hydrogen and oxygen atoms involved in hydrogen bonding in terms of the AIM theory of Bader.[20]

In this paper we have concentrated on measurements of the ^{17}O isotropic shielding (chemical shift) for water molecules in binary diol−water mixtures as a means of investigating changes in the electronic environment of the oxygen nucleus. Hydrogen bonding is manifest in changes in chemical shift which reflect alterations in the coupling constant, the EFG asymmetry parameter, and electron density experienced by the nucleus. We interpret the downfield shift seen for type II diols as consistent with increased time-averaged hydrogen bonding for solvent water and the initial slope as a direct reflection of the stoichiometry for this interaction. The magnitude of this initial downfield shift (1.0−1.5 ppm) should be compared to the downfield shift for water on going from 100 to 0 °C (∼5 ppm); it is equivalent, as far as the oxygen nucleus is concerned, to reducing the temperature by about 30 °C.

It is necessary to be clear on the differences between the two models—the *B*-coefficient relaxation rate or dynamic hydration number (DHN) model and our chemical shift (CS) model. It is clear that the DHN model probes water motion and the changes brought about by the addition of solute. The evidence for a specific type II diol effect on chemical shift, interpreted as an effect on hydrogen bonding, is also clear. We have been unable, however, to demonstrate any structurally specific effect of type II diols on spin−lattice relaxation or self-diffusion rates for water [Klein and Pacheco, unpublished work to be submitted], suggesting that the downfield shift seen for the $CH_3CH(OH)-$ group is not associated with measurable changes in motional correlation times. We would postulate that the methylcarbinol group produces structuring of solvent water in the vicinity of the methyl group—it is known that stable hexahydrates are formed with this type of compound—by bringing about a network of hydrogen bonds in a cooperative manner, resulting in motional characteristics for individual water molecules that are not measurably different from bulk water but with a

paramagnetic contribution to the chemical shielding tensor that results in a downfield shift. One would expect such a cooperative network of hydrogen bonds to show enthalpy−entropy compensation and for the effects on electronic environment experienced by the $H_2{}^{17}O$ nucleus to show reinforcement where the water simultaneously acts as both hydrogen-bond donor and acceptor.[21]

The behavior of the (α,ω)-diols highlights differences between the DHN and CS models. The α,ω-diols ($n = 2-6$) produce an increasing upfield shift for $H_2{}^{17}O$, equivalent to a destructuring effect or weakening of the solvent water hydrogen bonds, with a magnitude approximately proportional to chain length as the possible spacing between the two hydroxyl groups increases (Table 1). This is quite contrary to what would be expected from determination of the *B* coefficients using spin−lattice relaxation rate measurements, in which the *B* coefficient and the dynamic hydration number are seen to increase on passing through the homologous series from ethane-1,2-diol to hexane-1,6-diol.[22] The polarity, however, decreases with chain length as judged from their dielectric constants (12EG = 41.4,[30] 13PD = 35.1;[30] 14BD = 31.9,[25] 15PD = 26.2,[20] and 16HD = 25.9[20]),[17] as does their solubility in water. Thus the *B* coefficients would seem to suggest that the less polar, longer chain (α,ω)-diols are more hydrated than their more polar, shorter chain counterparts. A similar trend is seen for the monohydric alcohols:[22] ethylene glycol appears to be less "hydrated" (DHN = 5.7) than ethanol (DHN = 10.5). Increasing dynamic hydration numbers tend to be associated with increasing molecular size, itself associated with increasing viscosity. One possible interpretation is that the DHN does not represent a hydration shell in the true sense, at least for nonelectrolytes, but rather the number of water molecules whose motional correlation time is influenced by the presence of solute.

It is now accepted that C−H groups may form weak hydrogen bonds of the C−H···O type and that these may be strongly influenced by their environment to the extent of showing cooperativity.[23−28] Although the ability of a C−H group to donate hydrogen bonds depends on hybridization, $C(sp^1)-H \gg C(sp^2)-H \gg C(sp^3)-H$, even the donor strength of $C(sp^3)-H$ can be enhanced or activated by adjacent electron-withdrawing groups to produce relatively strong hydrogen bonds. Ab initio calculations yield equilibrium hydrogen-bond energies for water as acceptor and various C−H donors of between −0.5 and −9.3 kcal/mol, with the weakly polarized, symmetrical CH_4 donor giving −0.5 to −0.6 kcal/mol, dominated by the van der Waals interaction. Hydrogen-bond strengths are, however, strongly influenced by their environment including other hydrogen bonds.[25] Donor−acceptor separation has been found to depend on carbon acidity, as measured in DMSO.[29]

We propose that the 11 ± 2 water molecules in type II diols associated with the $CH_3CH(OH)-$ group could form a cage- or clathrate-like structure consisting of a partial face-centered pentagonal dodecahedron around the hydrophobic methyl group, as observed crystallographically for the methyl groups of Leu-18 in the protein crambin by Teeter[30] and for pinacol (2,3-dimethyl-2,3-butanediol) hexahydrate by Kim and Jeffrey,[31] who point out that a hexahydrate has also been reported for *meso*-2,3-butanediol as well for other methylated 2,3-butanediols and 2,5-dimethyl-2,5-hexanediol. In the case of crambin Teeter observed puckered clusters of pentagonal arrays of 16 waters surrounding the leucine methyl groups; Kim and Jeffrey measured O···O distances of 2.822 Å in the water layer around pinacol. Graphical analysis of the data reported by Anderson and Symons for TBA−water mixtures[12] yields a stoichiometry of 15−20 water molecules per alcohol molecule, rather more than we observed for the diols 12PG, 13BD, 23BD, 24PD, and 25HD. This is not altogether surprising as the $(CH_3)_3C-$ group is larger and could accommodate more water molecules through the formation of weak hydrogen bonds.

Both the methyl carbon and oxygen atoms in the $CH_3CH(OH)-$ group are significantly deshielded as evidenced by experimental NMR measurements[32,33] and based on theoretical ab initio calculations we have carried out at the MPW1PW91/6-311+G(2d,p) level.[34] The methyl carbon of the $CH_3CH(OH)-$ group may become shifted by as much as 50−60 ppm downfield from a normal alkyl chain methyl group, depending on structure. The oxygen resonance is also shifted downfield by about 30−40 ppm both experimentally using NMR and based on theoretical calculations in comparison to the hydroxyl oxygen in straight-chain (α,ω)-diols. Secondary alcohols, with substituent alkyl chains longer than methyl, show much reduced downfield shifts. Thus the available evidence indicates that the average electron density at both the methyl carbon and oxygen atoms may be reduced or the asymmetry increased, given the stricture expressed above that we are dealing with single-bonded oxygen, rather than being increased at the oxygen atom as classical inductive theory would suggest,[35] the explanation assumed by MacFarlane and Forsyth[36,37] to lead to increased basicity and stronger hydrogen-bond formation. It is worth noting, however, that Forsyth and MacFarlane[36] did not make measurements of the H_2O proton chemical shift in the region where the glycol was in dilute solution, but reported data for glycol concentrations greater than 20 mol %.

The deshielding of the methyl carbon and oxygen atoms, associated with a possible reduction in electron density and changes in asymmetry parameter, could be seen as a mechanism for "activating" these atoms, making it easier to abstract a proton and hence increasing their potential as hydrogen-bond donors,[25] rather than as hydrogen-bond acceptors as implied by MacFarlane and Forsyth. Hydrogen-bond formation between water molecules results in further downfield shifts, i.e., a further reduction in oxygen electron density and an increase in asymmetry. In forming a loosely bonded or "soft" cage containing 11 ± 2 waters molecules surrounding the $CH_3CH(OH)-$ group, one can envisage a cooperative network of adjacent water molecules resulting in an average bonding energy of −1 to −2 kJ/mol (−300 to −500 cal/mol), based on the experimentally determined Arrhenius enthalpy, ΔH, of between −13 and −17 kJ/mol (−3 to −4 kcal/mol). Based on the values quoted by Steiner,[25] this would correspond to individual hydrogen bonds being classified as very weak, but this could be considered to be offset by the cooperativity of the whole ensemble yielding a total enthalpy of around −15 kJ/mol. The complete lack of temperature sensitivity for the destructuring effects of type I diols is more difficult to explain. It is possible, however, that these diols destroy the cooperativity of long-range water networks, i.e., clusters, without net change in enthalpy, at least within experimental error. Further work is being carried out to elucidate this phenomenon.

Biological Relevance. There may be biological and biochemical relevance to these observations, apart from the stabilization of structural water in proteins such as crambin. The amino acid threonine contains the $CH_3CH(OH)-$ group as a side chain. Threonine is considerably more polar than might be expected given the presence of a methyl group, with a transfer energy similar to that of glycine.[38] Moreover, it is rarely if ever found in enzyme active centers, although the reasons for this may be predominantly steric in origin. Furthermore, threonine

is an important component of the glycosylation triplet in glycoproteins and is implicated in the mechanism of glycosylation[39] by the enzyme oligosaccharyltransferase: the electronic properties of the 3-OH oxygen atom are thought to be critical to the catalytic mechanism. Deoxyhexoses contain this group as a synthon within the ring system; fucose (6-deoxy-galactose) is important as an antigenic determinant in complex carbohydrates, whereas rhamnose (6-deoxy-mannose) occurs in plants and may be involved in protection against freezing. In both cases it is tempting to speculate that the structuring of water molecules around the methyl group β to an oxygen atom may be important. Formation of a clathrate-like cage of water molecules may also be important as a mechanism for explaining the effectiveness of 2,3-butanediol as a cryoprotectant in suppressing ice-crystal formation and encouraging vitrification in aqueous solutions, this diol being nearly twice as effective on a concentration basis as 1,2-ethanediol.[37,40] Thus the formation of "soft" ice around the $CH_3CH(OH)-$ group stabilized by weak C−H···O interactions and the presence of the OH group prevents the formation of true ice and allows vitrification rather than crystallization.

Acknowledgment. We acknowledge financial assistance in the form of a project grant from the Deutsche Forschungsgemeinschaft (DFG SFB 284/A1) and from the Central University of Venezuela and Conicit, Venezuela.

References and Notes

(1) Jonsdottir, S. O.; Klein, R. A.; Rasmussen, Kj. *Fluid Phase Equilib.* **1996**, *115*, 59.

(2) Jonsdottir, S. O.; Klein, R. A. *Fluid Phase Equilib*. **1997**, *132*, 117.

(3) Jonsdottir, S. O.; Rasmussen, P. *Fluid Phase Equilib.* **1999**, *158*−*160*, 411.

(4) Jonsdottir, S. O.; Welsh, W. J.; Rasmussen, Kj.; Klein, R. A. *New J. Chem*. **1999**, 153.

(5) Glasel, J. A. Nuclear Magnetic Resonance Studies on Water and Ice. In *Water*−*a Comprehensive Treatise*; Franks, F., Ed.; Plenum Press: New York & London, 1982; Vol. 1, Chapter 6, p 223. Fister, F.; Hertz, H. G. *Ber. Bunsen-Ges. Phys. Chem.* **1967**, *71*, 1032. Hertz, H. G.; Maurer, R.; Killie, S. *Z. Phys. Chem.* **1991**, *172* (2), 157. Luz, Z.; Yagil, G. *J. Phys. Chem.* **1966**, *70*, 554.

(6) Wasylishen, R. E.; Mooiibroek, S.; Macdonald, J. B. *J. Chem. Phys.* **1984**, *81* (3), 1057. Wu, G.; Hook, A.; Dong, S.; Yamada, K. *J. Phys. Chem. A* **2000**, *104*, 4102.

(7) Moriarty, N. W.; Karlström, G. *Chem. Phys. Lett.* **1997**, *279*, 372.

(8) Marquardt, D. W. *J. Soc. Ind. Appl. Math.* **1963**, *11*, 431.

(9) Press, W. H.; Teukolsky, S. A.; Vetterling, W. T.; Flannery, B. P. *Numerical Recipes in C*−*the Art of Scientific Computing*; 2nd ed.; Cambridge University Press: Cambridge, UK, 1995; p 683.

(10) Motulsky, H. *Analyzing Data with GraphPad Prism*; GraphPad Software, Inc.: San Diego, CA, 1992, 1999; p 167.

(11) Glew, D. N.; Mak, H. D.; Rath, N. S. *Chem. Commun.* **1968**, 264.

(12) Anderson, R. G.; Symons, M. C. R. *Trans. Faraday Soc.* **1969**, *65*, 2550.

(13) Blandamer, M. J.; Clarke, D. E.; Claxton, T. A.; Fox, M. F.; Hidden, N. J.; Oakes, J.; Symons, M. C. R.; Verma, G. S. P.; Wootten, M. J. *Chem. Commun.* **1968**, 273.

(14) Burgess, J. *Chem. Commun*. **1967**, 1134.

(15) de Visser, C.; Perron, G.; Desnoyes, J. E. *Can. J. Chem.* **1977**, *55*, 856.

(16) Tanford, C. *The Hydrophobic Effect: Formation of Micelles and Biological Membranes*, 2nd ed.; John Wiley & Sons: New York, 1980.

(17) Wohlfarth, C. In *CRC Handbook of Chemistry and Physics*, 77th ed.; Lide, D. R., Frederikse, H. P. R.; Eds.; CRC Press: Boca Raton, 1996−1997; p 6-151.

(18) Murthy, S. S. N. *Cryobiology* **1998**, *36*, 84.

(19) Bagno, A.; Lovato, G.; Scorrano, G.; Wijnen, J. W. *J. Phys. Chem.* **1993**, *97* (18), 4601. van der Maarel, J. R. C.; Lankhorst, D.; de Bleijser, J.; Leyte, J. C. *J. Phys. Chem*. **1986**, *90* (7), 1470.

(20) Bader, R. F. W. *Atoms in Molecules. A Quantum Theory*; Oxford University Press: Oxford, 1990. See, for example: Pacios, L. E.; Gómez, P. C. *J. Comput. Chem.* **2001**, *22* (7), 702.

(21) Calderone, C. T.; Williams, D. H. *J. Am. Chem. Soc.* **2001**, *123* (26), 6262. Mó, O.; Yanez, M.; Elguero, J. *J. Chem. Phys.* **1992**, *97*, 6628. Masella, M.; Flament, J.-P. *J. Chem. Phys.* **1999**, *111*, 5081. King, B. F.; Weinhold, F. *J. Chem. Phys.* **1995**, *103*, 333.

(22) Ishihara, Y.; Okouchi, S.; Uedaira, H.; *J. Chem. Soc., Faraday Trans.* **1997**, *93* (18), 3337.

(23) Taylor, R.; Kennard, O. *J. Am. Chem. Soc.* **1982**, *104*, 5063.

(24) Steiner, T.; Saenger, W. *J. Am. Chem. Soc.* **1992**, *114*, 10146.

(25) Steiner, T. *Chem. Commun.* **1997**, 727.

(26) Steiner, T.; Lutz, B.; van der Maas, J.; Veldman, N.; Schreurs, A. M. M.; Kroon, J.; Kanters, J. A. *Chem. Commun.* **1997**, 191.

(27) Steiner, T. *New J. Chem.* **1998**, 1099.

(28) Desiraju, G. R.; Steiner, T. *The Weak Hydrogen Bond in Structural Chemistry and Biology*; International Union of Crystallography Monographs on Crystallography 9; Oxford University Press: Oxford, UK, 1999; p 507.

(29) Pedireddi, V. R.; Desiraju, G. R. *J. Chem. Soc., Chem. Commun.* **1992**, 988.

(30) Teeter, M. M. *Proc. Natl. Acad. Sci. U.S.A.* **1984**, *81*, 8014.

(31) Kim, H. S.; Jeffrey, G. A. *J. Chem. Phys.* **1970**, *53* (9), 3610.

(32) Crandall, J. K.; Centeno, M. A. *J. Org Chem.* **1979**, *44* (7), 1183.

(33) Grindley, T. B.; Cote, C. J. P.; Wickramage, C. *Carbohydr. Res.* **1985**, *140*, 215.

(34) Klein, R. A.; Pacheco, V. Data to be reported elsewhere.

(35) Sykes, P. *A Guidebook to Mechanism in Organic Chemistry*, 6th ed., Longman: London, 1986.

(36) Forsyth, M.; MacFarlane, D. R. *J. Phys. Chem.* **1990**, *94* (17), 6889.

(37) MacFarlane, D. R.; Forsyth, M. *Cryobiology* **1990**, *27*, 345.

(38) Engelman, D. M.; Steitz, T. A.; Goldman, A. *Annu. Rev. Biophys. Biophys. Chem.* **1986**, *15*, 330.

(39) Bause, E., Breuer, W., Peters, S. *Biochem. J.* **1995**, *312*, 979.

(40) Fahy, G. M.; Levy, D. I.; Ali, S. E. *Cryobiology* **1987**, *24*, 196.